Sādhanā (2022)47:82
https://doi.org/10.1007/s12046-022-01858-7

Constitutive modeling for the tear fracture of rubber with filler particles

SANKALP GOUR, DEEPAK KUMAR* and VINOD YADAV

Department of Mechanical Engineering, Maulana Azad National Institute of Technology Bhopal, Bhopal 462003, Madhya Pradesh, India
e-mail: deepakkumaromre@manit.ac.in

MS received 24 September 2021; revised 21 December 2021; accepted 11 February 2022

Abstract. This work presents the constitutive modeling for the tear fracture and its mechanical behavior of rubber with filler particles. A continuum mechanics-based analytical model is developed here to predict the mechanical properties of rubber with a suitably added filler. The model is then validated with the experimental results of the chloroprene and nitrile butadiene rubbers filled with different volume fractions of carbon black and carbon nanoparticles, respectively. Further, the tear fracture phenomenon of the filled rubber is modeled adopting a well-known Griffith criterion based on the developed constitutive model. The aimed tear fracture phenomenon is focused on a particular fracture test of mode-III, namely the trousers test, where two legs of a cut specimen are pulled horizontally apart. The results show that the fracture toughness of the filled rubber increases with the rise in the volume of filler particles. In general, the developed model will be helpful to the researchers in characterizing the material behavior of tires and other rubber-like materials.

Keywords. Continuum mechanics; constitutive modeling; elastomeric material; filled rubber; tear fracture; fracture toughness.

1. Introduction

Rubber or rubber-like material is a long-chain polymer with minor impurities of other organic compounds. A polymer that exhibits rubber-like elasticity is also referred to as elastomer, or sometimes rubber elastomer [1]. These rubber elastomers have high availability, and low raw material cost with the most desirable property of large deformations under small stresses [2, 3]. Examples of such rubber elastomers are the chloroprene and nitrile butadiene rubbers that can be reinforced with different volume fractions of carbon and carbon nanotube particles, respectively, to alter their material properties. Both unfilled and filled rubber elastomers hold an important place within the rubber industry, in high demand by manufacturers. The difference between unfilled and filled rubber elastomers makes both types useful for different applications. The polymeric or elastomeric materials obey a continuum mechanics-based hyperelastic theory in which the stress-strain relationship is derived from a specially defined strain energy density function [4–8]. In general, polymeric materials have been used in diverse applications such as vibration isolation, structural bearings, tires, biomechanics, gaskets, engine mounts, etc [9–12]. In addition, fillers play vital roles in transforming the desirable properties of polymers and decreasing the overall cost of their composites. Sometimes, in various applications, the elastomers may get teared due to some unknown reasons. Therefore, the study on the tear fracture of the filled and unfilled rubber elastomers becomes so essential in rubber-based product manufacturing industries.

To mention some earlier works on the filled rubber elastomers, several researchers [13–15] have experimented the elastomers with different volume fractions of filler materials. They observed the possibility of inducing elastomeric properties by varying the filler particles' volume fraction, shape, and size. A further enhancement was also acquired by the use of filler materials with higher aspect ratios, like short glass fibers [16–20]. Such fillers particles include layered silicates and carbon nanotubes [21, 22]. Later, a limited number of authors, namely Reichert *et al* [23], Farris [24] and Berriot *et al* [25] attempted the constitutive modeling developments of elastomers with filler particles. In line with that, Reichert *et al* [23] proposed a double network-based model by writing the total stress as a superposition of stresses of the individual networks to describe filled elastomers. Next, Farris [24] modeled the influence of vacuole formation on the response and failure of filled elastomers providing a method for determining the extent of microscopic failure within the material. Further, Berriot *et al* [25] modeled elastomeric interaction with fillers based on the 1H-NMR unresolved nuclear magnetic

*For correspondence
Published online: 20 April 2022

resonance (NMR) experiments. He studied the effect of filler particles on the network structure of the elastomer with chain mobility at the interface. Furthermore, Leonard *et al* [26] reported a computational method to model the polydimethylsiloxane (PDMS) elastomer with prototypical added fillers by excluding the presence of inter-phases and occluded rubber mechanisms.

The present study aims to apply the constitutive modeling results in the tear fracture phenomenon of rubber-like materials with different volume fractions of filler particles. For the same, a particular fracture test, namely the trousers test [27–29], is focused, wherein two legs of a cut specimen are pulled horizontally apart. To the best of our knowledge, an analytical modeling of the aimed tearing phenomenon of filled elastomers is motivated here for the first time in the literature. However, a very few analytical works [27, 28, 30, 31] on the tear fracture of rubber elastomers have been performed, which are limited for the unfilled rubber elastomers only. The utility of the hyperelastic constitutive models is investigated here in predicting some features of filled-rubber fracture of mode-III (tearing mode).

The organization of the paper is as follows. In section 2, a constitutive model is developed to describe the nonlinear elastic response of the various particle-reinforced rubber elastomers. In section 3, the analytical and experimental results are compared and analyzed. In section 4, the tearing phenomenon based on trousers test for rupture is analytically modeled and analyzed. Finally, section 5 concludes the article.

2. Constitutive modeling

In this section, an analytical model for the mechanical behavior of rubber with filler particle is developed. To develop the same, a continuum mechanics-based hyperelasticity theory is adopted.

2.1 *Problem description and material deformation*

Consider a particle-filled rubber elastomer sample having the dimensions (L_1, L_2, L_3) in the reference configuration β_0 shown in figure 1. A compressive force P is applied on the rubber sample to deform the same for the deformation analysis. The deformed rubber sample is now having the dimensions (l_1, l_2, l_3) in the current configuration β. Herein, the observations are being made on the macro-scale. The material continua of a particle-filled rubber sample is assumed to be incompressible, isotropic, and homogeneously filled with the filler content. For a given deformation of an applied compressive force, the problem aims to derive an expression of the constitutive relationship between stress and deformation, including the volume fraction of filler particles following a classical continuum mechanics-based approach.

The domain occupied in a 3-D space by a rubber sample shown in figure 1 may be represented as

$$\begin{aligned}\beta_0 = [\mathbf{X} \in \Re^3 : \frac{-L_1}{2} \le X_1 \le \frac{L_1}{2}, \quad \frac{-L_2}{2} \le X_2 \le \frac{L_2}{2}, \\ \frac{-L_3}{2} \le X_3 \le \frac{L_3}{2}], \\ \beta = [\mathbf{x} \in \Re^3 : \frac{-l_1}{2} \le x_1 \le \frac{l_1}{2}, \quad -\frac{-l_2}{2} \le x_2 \le \frac{l_2}{2}, \\ \frac{-l_3}{2} \le x_3 \le \frac{l_3}{2}].\end{aligned} \tag{1}$$

For a given reference β_0 and current configuration β domains in the above equation (1), the stretches in the principal direction may be defined as

$$\lambda_1 = \frac{l_1}{L_1}, \quad \lambda_2 = \frac{l_2}{L_2}, \quad \lambda_3 = \frac{l_3}{L_3}. \tag{2}$$

On using the incompressibility constraint $\lambda_1\lambda_2\lambda_3 = 1$, the principal stretches for an uniaxial compression of the rubber sample are given as

$$\lambda_1 = \lambda, \quad \lambda_2 = \frac{1}{\sqrt{\lambda}}, \quad \lambda_3 = \frac{1}{\sqrt{\lambda}}, \tag{3}$$

where λ denotes the stretch in the direction of applied load. The deformation gradient tensor $\mathbf{F}$ and the corresponding left-Cauchy green deformation tensor $\mathbf{B} = \mathbf{F}\mathbf{F}^T$ for an uni-axial compression of the rubber sample having the

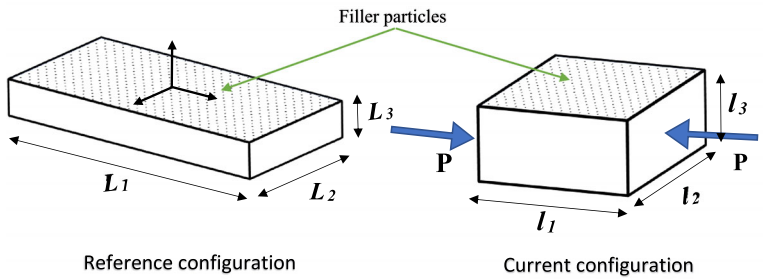

Figure 1. Schematic diagram of a rubber sample with filler particles in undeformed and deformed configurations.

deformation domain (1) in terms of principal stretches are defined as

$$\mathbf{F} = \begin{bmatrix} \lambda & 0 & 0 \\ 0 & \frac{1}{\sqrt{\lambda}} & 0 \\ 0 & 0 & \frac{1}{\sqrt{\lambda}} \end{bmatrix}, \quad \mathbf{B} = \begin{bmatrix} \lambda^2 & 0 & 0 \\ 0 & \frac{1}{\lambda} & 0 \\ 0 & 0 & \frac{1}{\lambda} \end{bmatrix}. \tag{4}$$

In general, it is easier and convenient to use the left Cauchy-Green tensor **B** compared to other measures of deformation, as it is free from rigid body rotation.

2.2 *Material modeling*

To model the mechanical behavior of rubber with filler particles, we first require an energy density function that can capture the effect of filler content on the shear modulus of the rubber matrix. For the same, we use a strain energy density function in line with the literature [32, 33] which includes the volume fraction term of the filler particles. The expression of the Neo-Hookean type of strain energy density function is given as

$$W = \frac{\mu}{2}(1 - v_f)(1 + 3.5v_f + 30v_f^2)(I_1 - 3), \tag{5}$$

where v_f, μ, and $I_1 = \lambda_1^2 + \lambda_2^2 + \lambda_3^2$ are the volume fraction of the added filler particle in the rubber matrix, shear modulus, and the first invariant of the left-Cauchy green deformation tensor **B**. So many energy functions exist to model the material properties of rubber-like materials. Out of these, the chosen Neo-Hookean energy density (5) has a linear function of the first strain-invariant only with a virtue of mathematical simplicity that facilitates the analytic solution of many fundamental boundary-value problems. From the theory of hyperelasticity [34, 35], the Cauchy stress tensor for a given strain energy density function W is expressed as

$$\mathbf{S} = -p\mathbf{I} + 2\frac{\partial W}{\partial I_1}\mathbf{B} - 2\frac{\partial W}{\partial I_2}\mathbf{B}^{-1}, \tag{6}$$

where p is a Lagrange multiplier associated with the constraint of incompressibility and I_1, I_2 are the first and second invariants of the left-Cauchy green deformation tensor **B**. On using the given filler particle volume dependent strain energy density function (5) in (6), the corresponding principal Cauchy stress components are obtained as

$$\begin{aligned} S_{11} &= -p + \mu(1 - v_f)(1 + 3.5v_f + 30v_f^2)\lambda^2, \\ S_{22} &= -p + \mu(1 - v_f)(1 + 3.5v_f + 30v_f^2)\frac{1}{\lambda}, \\ S_{33} &= -p + \mu(1 - v_f)(1 + 3.5v_f + 30v_f^2)\frac{1}{\lambda}. \end{aligned} \tag{7}$$

On applying uni-axial compression boundary conditions, i.e., $S_{11} = \sigma$, $S_{22} = S_{33} = 0$ in (7), the Cauchy or true stress σ in the applied load direction is obtained as

$$\sigma = \mu(1 - v_f)(1 + 3.5v_f + 30v_f^2)\left(\lambda^2 - \frac{1}{\lambda}\right). \tag{8}$$

The above constitutive relation (8) represents a continuum mechanics-based analytical model to predict the experimentally observed mechanical behavior of the filler particles reinforced rubber elastomers.

3. Experimental validation of the model

In this section, the constitutive model presented in section 2 is compared and validated with the chloroprene and nitrile butadiene rubbers data filled with different volume fractions of carbon and carbon nanotube particles, respectively. It is also utilized in characterizing the mechanical behavior of the same.

3.1 *Model validation with chloroprene rubber data filled with different percentages of carbon black*

To check the validity of the model (8) presented in section 2, we compare our theoretical findings with the experimental work performed by Bergstrom and Boyce [36]. He performed several compression tests to study the stress-strain behavior of a chloroprene rubber at different volume fractions of N600 carbon black. The testing was done on a computer controlled Instron servo-hydraulic uniaxial testing machine operating in strain control mode. The tested specimens used were ASTM-sized, with a height and diameter of 13 mm and 28 mm, respectively. We analyze the experimental results [36] and obtain similar findings analytically utilizing the developed model (8). To compare analytical and experimental data, we plot and validate the Cauchy stress versus stretch curves for a chloroprene rubber with varied N600 carbon black filler content shown in figure 2.

By fitting the model (8) with experimental data [36] shown in figure 2, we tabulate the shear modulus μ values in table 1 at different percentages of carbon black added in a chloroprene rubber. A well-known method of least-squares [37] is adopted here for fitting the model (8) with experimental data [36]. In table 1, the carbon black content variations from 0 to 7 %, 7 to 15%, and 15 to 25% lead to an increase in the chloroprene rubber's shear modulus 48.48% , 17.34%, and 0.52%, respectively. Consequently, it is observed that the addition of the carbon particles in the rubber matrix increases the shear modulus up to a certain value. It is further observed from here that the percentage effect of filler content is more pronounced at a high stretch

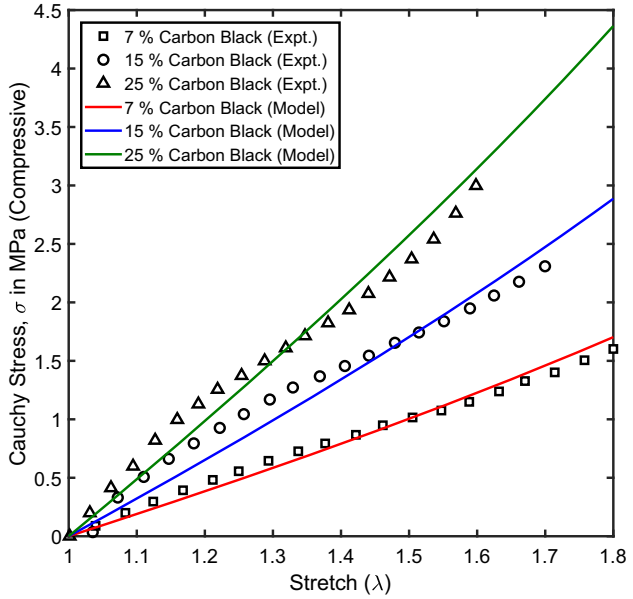

Figure 2. Validation of the model (8) with Bergstrom and Boyce experimental data [36] for a chloroprene rubber filled with different levels of N600 carbon black.

Table 1. Shear modulus values for a chloroprene rubber at different percentages of added carbon black filler particles.

Carbon Black (v_f)	Shear Modulus (μ)	R-square
0 %	330 kPa	–
7 %	490 kPa	0.9824
15 %	575 kPa	0.9512
25 %	578 kPa	0.9737

than a low stretch. Also, the variation of Cauchy stress with the stretch is almost linear. However, the slope in each case of different filler particles is varied. Thus, the dependency of the proposed model (8) is highly desirable on the shear modulus of the specified rubber filled with carbon black. Physically, an increase in the volume fraction of filler particles reduces the deformation tendency of polymeric chains of rubber elastomers by decreasing the entropy level of chains. These physical changes in the rubber elastomers result in an enhanced shear modulus of the material.

3.2 *Model validation with nitrile butadiene rubber data filled with different percentages of carbon nano particle*

To further assess the validity of the model (8), we compare the analytical findings with the experimental work performed by Mahmoud *et al* [38]. He experimentally characterized the mechanical behavior of the nitrile butadiene rubber (NBR) by adding carbon nanoparticles (CNPs). The testing nanocomposite material was in the form of strips as per the ASTM D 412-8a standards having length 0.3 m and radius 0.15 m. The testing was done on a computer-controlled material testing machine (AMETEK, USA) connected by a digital force gauge (Hunter Spring AC-CU Force II, 0.01-Nresolutions) to estimate the forces. We re-analyze the experimental results [38] and obtain similar findings analytically utilizing the model (8). To make a comparison between the analytical and experimental results, we plot and validate the Cauchy stress versus stretch curves for a nitrile butadiene rubber filled with different levels of carbon nanoparticles shown in figure 3.

Following the method of least-squares [37], as mentioned earlier, we tabulate the corresponding values of shear modulus μ in table 2 at different percentages of carbon nanoparticles filled in a nitrile butadiene rubber. In table 2, the carbon nanoparticles content variation from 0 to 0.7% and 0.7 to 1.3% lead to an increase in the shear modulus of the nitrile butadiene rubber 203% and 66.67%, respectively. Further, the carbon nanoparticles content variation from 2 to 2.6%, 2.6 to 3.3%, respectively, observe 39.58% and 7.46% increase in the shear modulus of the nitrile butadiene rubber. Interestingly, the carbon nanoparticles content variation from 0 to 3.3 % shows a jump in the shear modulus by 1354 % theoretically. On the other hand, an increase in shear modulus rate is observed low with increasing the percentage content of carbon nanoparticles in the nitrile butadiene rubber. Hence, the combined effect of increasing the carbon nanoparticles along with the shear modulus is studied underpin. Also, an increase in the carbon nanoparticle content steepers the Cauchy stress-

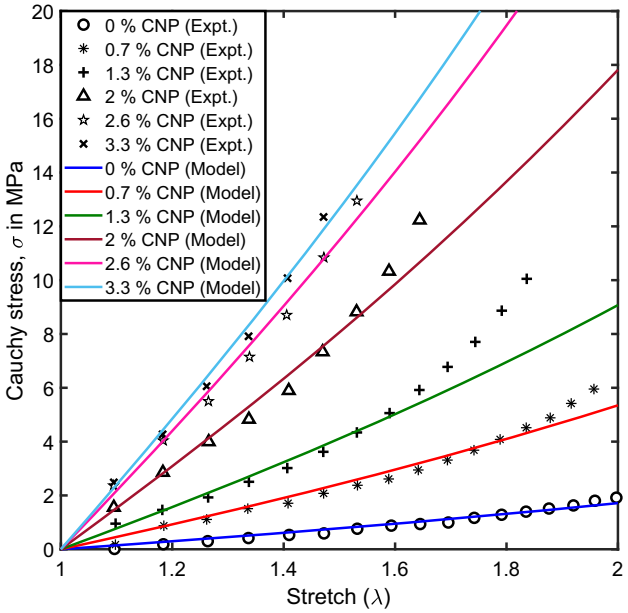

Figure 3. Validation of the model (8) with Mahmoud et al. experimental data [38] for a nitrile butadiene rubber (NBR) filled with different levels of carbon nanoparticles (CNPs).

Table 2. Shear modulus values for a nitrile butadiene rubber (NBR) at different percentages of added carbon nanoparticles (CNPs).

Carbon Nano Particles (v_f)	Shear Modulus (μ)	R-square
0 %	495 kPa	0.9651
0.7%	1500 kPa	0.9654
1.3%	2500 kPa	0.9271
2 %	4800 kPa	0.9706
2.6 %	6700 kPa	0.9872
3.3 %	7200 kPa	0.9918

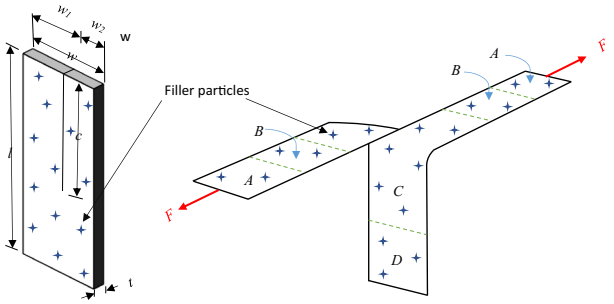

Figure 4. Schematic diagram of trousers test specimen.

stretch curves, as shown in figure 3. This may be due to an increase in the shear modulus of the rubber matrix. Physically, this means that the deformation tendency of polymeric chains in NBR reduces with an increase in the CNPs, resulting in NBR being more stiffer. Furthermore, the stretch abilities of the rubber are reduced significantly in line with the experimental data [38].

4. Tear fracture of filled rubber

In this section, a theoretical modeling framework is presented for the tear fracture of filled rubber at different ratios of filler particles. The aimed modeling framework is inspired by an analytical treatment of a commonly used trousers test for rupture [27, 28] to investigate the fracture of elastomers. A well-known Griffith criterion for the failure of an elastomer outlined in [27] is adopted here. The tearing phenomenon of filled rubber is investigated using the trousers test for rupture utilizing the constitutive model (8) presented in section 2. In general, the Griffith criterion talks about the tear behavior of the rubber in accordance with the potential energy release rate as the crack grows in the rubber elastomer [27, 39]. It was initially explored by Irwin [40] for a plastic deformation of the metals. Later, Rivlin and Thomas [41] extended the same for the analysis of cut growth in a vulcanized rubber sheet.

Consider a test specimen having length l, width w, thickness t as shown in figure 4 followed by the standards mentioned in [27]. The specimen is then cut with a length c along the axial direction. The position of the cut divides the width of the specimen into two legs of width w_1 and w_2 (such that $w = w_1 + w_2$, where w is the total width of the specimen). In general, the position of the cut plays a vital role in the test outcomes. Further, both the legs are clamped and subjected to a constant tensile force F in the opposite directions. The applied force F leads to deformation in different regions of the test specimen shown in figure 2. The force F is applied to region A, which leads region B in a simple extension state. Next, region C describes a critical region in which the tearing phenomenon is observed. At last, region D shows the undeformed region. Later, the applied tensile force F is intensified up to a catastrophic increase in the crack length δc, which is recognized to compute the tearing energy E relating to the critical driving force.

Now, we examine region B for a simple extension case and use the results in the earlier sections. Sawyers and Rivlin [27] employed the Griffith criterion [41] for the failure to establish the following relation for the trousers test

$$F(\lambda_1 + \lambda_2) - t\left(w_1 W|_{\lambda=\lambda_1} + w_2 W|_{\lambda=\lambda_2}\right) = Et, \tag{9}$$

where w_1 and w_2 are the widths of leg 1 and leg 2 of the test specimen respectively, λ_1 and λ_2 are the principal stretches of leg one and two respectively, t is the thickness, F is the critical driving force, W is the potential energy function, and E is the tearing energy. Defining a dimensionless quantity ζ to denote the position of cut, we have

$$w = w_1 + w_2, \quad \zeta = \frac{w_1}{w}, \quad w_2 = (1-\zeta)w, \tag{10}$$

and the relation (9) simplifies to

$$F(\lambda_1 + \lambda_2) - tw\left[\zeta W|_{\lambda=\lambda_1} + (1-\zeta)W|_{\lambda=\lambda_2}\right] = Et. \tag{11}$$

For the given data of w, t, E, ζ, and W, the corresponding data of λ_1, λ_2 and F may be obtained. Application of forces on both the legs of the clamped specimen at equilibrium condition generates the net force constraint in each leg that must be equal. The force here in any rectangular section is defined as $F = S_{11}wt$ (where S_{11} is engineering stress), and using the model (8), we may attain the stretch relationship between both the legs for the employed energy density (5)

$$\begin{aligned}\frac{F}{\mu wt} &= \zeta(1-v_f)(1+3.5v_f+30v_f^2)\left(\lambda_1 - \frac{1}{\lambda_1^2}\right)\\ &= (1-\zeta)(1-v_f)(1+3.5v_f+30v_f^2)\left(\lambda_2 - \frac{1}{\lambda_2^2}\right).\end{aligned} \tag{12}$$

The relationship between stretches in both legs λ_1 and λ_2 using equation (12) at a middle cut position of the specimen

$\zeta = 0.5$ is illustrated in figure 5. A simple straight line curve (λ_1=λ_2) with an inclination of 45^o is noted here. Interestingly, it is observed that the stretch relationship is independent of the volume fraction of added filler particles. The volume fraction of added filler particles affects only the rubber stiffness and is independent of the cut position in the region of stretches of legs 1 and 2. However, for cut positions close to the edge, the value of stretch in leg 1 initially increases much faster than leg 2. Also, the cut position decreases as the width of one leg decreases, and for a smaller value of stretch in leg 2 (λ_2), a larger value of stretch in leg 1 (λ_1) is recognized.

Now, we may rewrite the relation (11) for the given energy density (5) to obtain the following trousers test of rupture relationship in a non-dimensional form

$$\frac{F}{\mu w t}(\lambda_1 + \lambda_2) - \frac{1}{2}(1 - v_f)(1 + 3.5v_f + 30v_f^2)$$
$$[\zeta(\lambda_1^2 + 2\lambda_1^{-1} - 3) + (1 - \zeta)(\lambda_2^2 + 2\lambda_2^{-1} - 3)] = \frac{E}{\mu w}, \tag{13}$$

where $F/\mu wt$ and $E/\mu w$ represent the non-dimensional critical driving force and non-dimensional fracture toughness, respectively. The critical driving force represents here the force encountered due to induced stress in hyperelastic rubber material. However, the fracture toughness describes the ability of the filled rubber to withstand the tearing energy before fracture, and it is evaluated in terms of the stress intensity. The critical driving force variation with the corresponding fracture toughness at different cut positions is illustrated in figure 6 for an unfilled rubber elastomer case ($v_f = 0\%$). Herein, the critical driving force for a known fracture toughness is lower at the nearby edge of the test specimen. On increasing the fracture toughness, the critical driving force gets enhanced with an increase in the cut positions. At the same time, for a fixed fracture toughness, the different values of the critical driving force are obtained on escalating the value ζ from 0.1 to 0.5.

Further, the critical driving force variation with the corresponding fracture toughness at different volume fractions of filler particles is illustrated in figure 7 for a filled rubber torn at a fixed position. Herein, significant growth of the critical driving force is observed with an increase in the fracture toughness for varying the volume fraction of added filler particles from 0% to 12%. Also, the excitation of the critical driving force is more pronounced for relatively higher fracture toughness values. At a particular fracture toughness (say $E/\mu w = 15$) with a defined cut position (say $\zeta = 0.1$), shown in figure 7(a), the critical driving force $F/\mu wt$ data are obtained as 1.6, 1.7, 2, and 2.5 for the given filler volume fractions v_f of 0%, 4%, 8%, and 12%, respectively. Furthermore, an increase in the cut position leads to a higher critical driving force, as shown in figures 7(b) and 7(c). For a given $v_f = 8\%$ volume fraction of added filler particles in the material, a 65% rise in the critical driving force is noted for an increase in the cut position from $\zeta = 0.1$ to $\zeta = 0.5$. Physically, an increase in the volume fraction of filler particles reduces the entropy level of the chain network that stiffens the elastomer. This reduced entropy structure of the elastomer resists tearing and creates a higher critical driving force requirement.

Figure 8 shows the fracture toughness variation with the cut position at different volume fractions of added filler

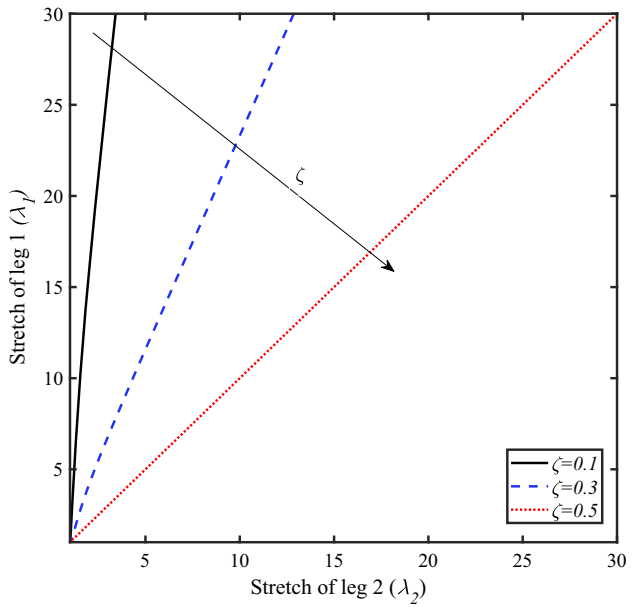

Figure 5. Relationship between stretch in legs 1 and 2 at different cut positions ζ.

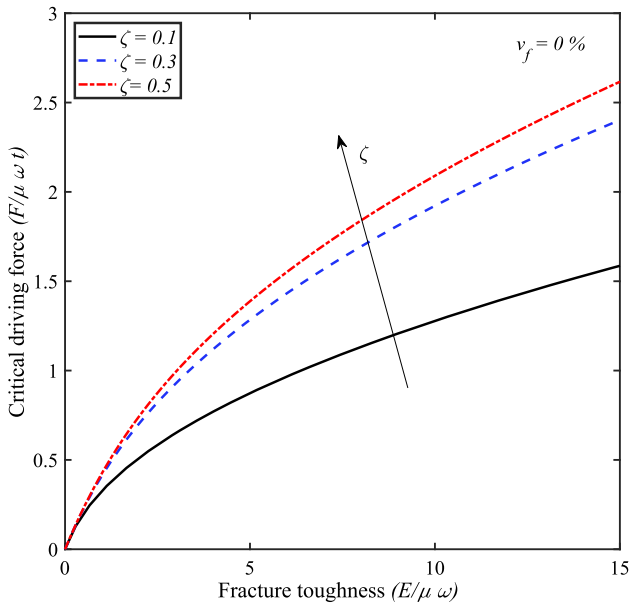

Figure 6. Critical driving force versus fracture toughness at different cut positions ζ for an unfilled rubber elastomer ($v_f = 0\%$).

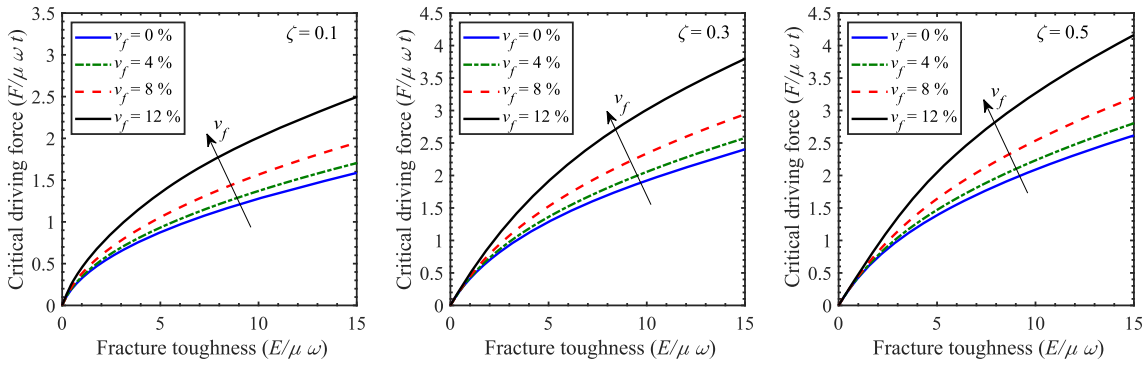

Figure 7. Critical driving force versus fracture toughness at different volume fractions of filler particles v_f for a fixed cut position (a) $\zeta = 0.1$, (b) $\zeta = 0.3$, and (c) $\zeta = 0.5$.

particles in the rubber matrix. Herein, increasing the volume of filler particles in the rubber makes the fracture toughness curve steeper with the cut position of the specimen. Also, an asymptotic nature of the curve is observed when the cut position approaches to edge of the test specimen (ζ tends to zero). At a particular cut position (say $\zeta = 0.1$) with a fixed stretch in leg 2 (say $\lambda_2 = 2$ or $\lambda = 4$), a decrease of 56.6% for $\lambda_2 = 2$ and 60.7% for $\lambda = 4$ in fracture toughness is noted for a given variation of the volume fraction of added filler particles from $v_f = 0\%$ to $v_f = 12\%$. An influence of cut position ζ has a higher impact on the fracture toughness than the volume fraction of filler particle, as we can note from equation (12). Therefore, an increase in the cut position ζ reduces the fracture toughness while increasing the volume fraction of filler particles.

Figure 9 describes the critical phenomena of a filled rubber elastomer having fixed cuts by varying the volume fractions of added filler particles on the fracture toughness versus critical driving force plot. The obtained critical curve here indicates the maximum fracture toughness of the material for a given volume fraction of the filler particles. With an increase in the cut position, the material fracture toughness rises significantly along with the critical driving force. Further, variation of the volume fraction of added filler particles in the rubber with a fixed cut position from $v_f = 0\%$ to $v_f = 12\%$ makes a decrease in the fracture toughness and the critical driving force. At last, an increase

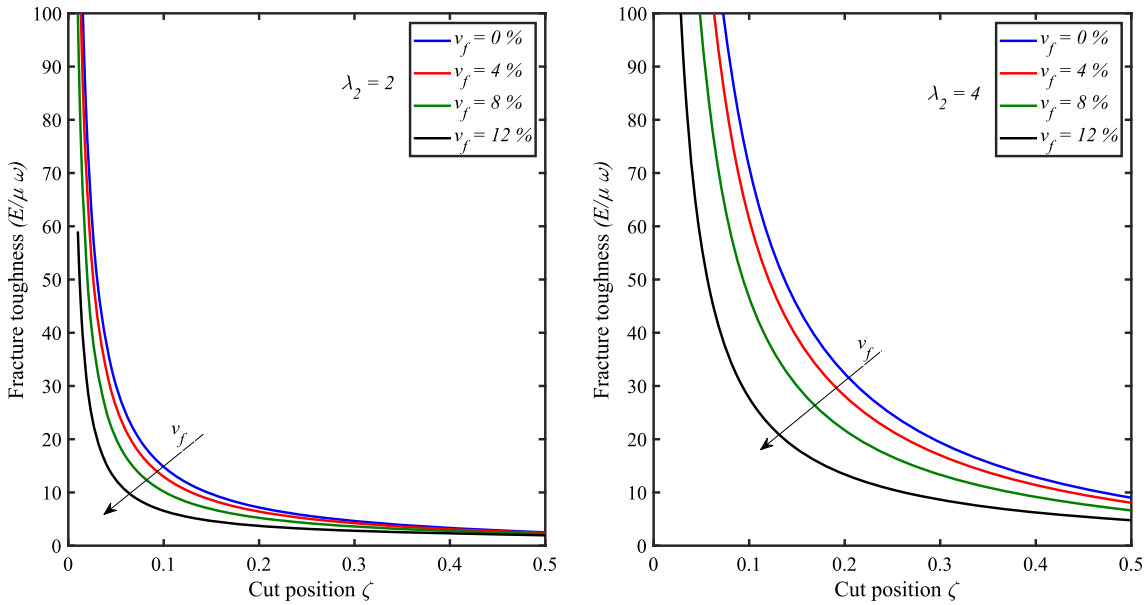

Figure 8. Fracture toughness versus cut position at different volume fractions of filler particles v_f for a fixed stretch (a) $\lambda_2 = 2$ and (b) $\lambda_2 = 4$ in leg 2.

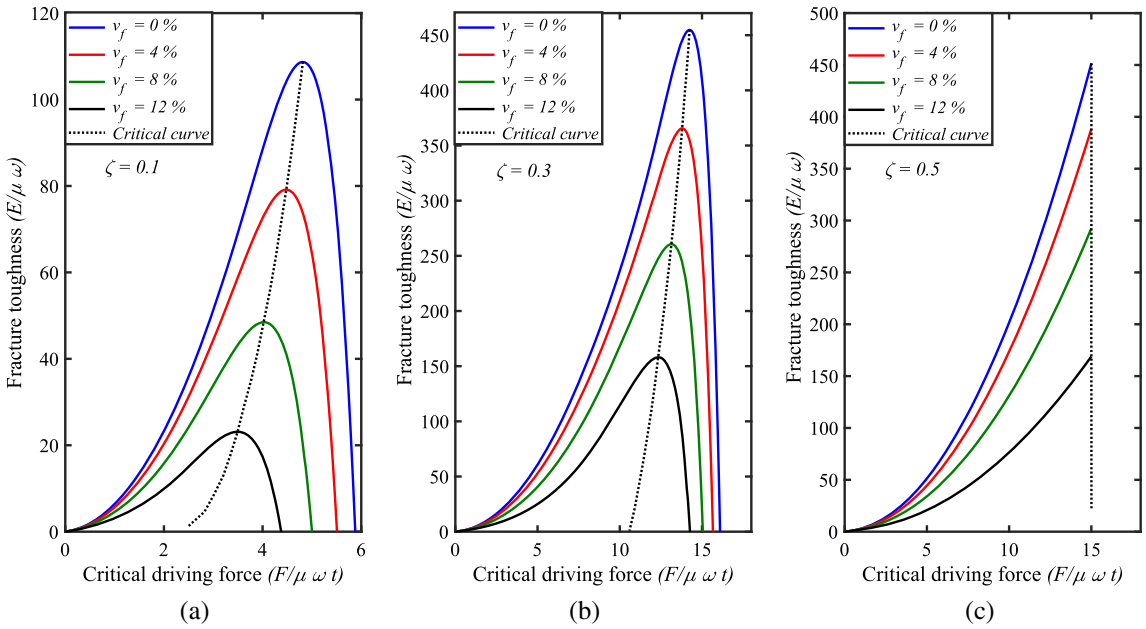

Figure 9. Fracture toughness versus critical driving force at different volume fractions of filler particles v_f for a fixed cut position (a) $\zeta = 0.1$, (b) $\zeta = 0.2$ and $\zeta = 0.5$.

in the cut width from the edge of the test specimen raises the slope of the critical curve that attains a maximum value at $\zeta = 0.5$ (shown as the chain dotted line in figure 9).

5. Concluding remarks

In this paper, an experimentally validated explicit expression of the Cauchy stress (8) is modeled by connecting the volume fraction of the added filler particles, shear modulus, and stretch for a given deformation in the direction of the applied load. The derived expression is then utilized to present a theoretical modeling framework for the tear fracture of filled rubber elastomers at different ratios of added filler particles. A well-known Griffith criterion for the failure is adopted here to model the aimed tear fracture phenomenon of the filled rubber elastomers focusing on a standard trousers test for the rapture. The proposed study articulates the following inferences:

- An enhancement in the mechanical properties of the rubber elastomers is possible by adding suitable filler particles to some extent.
- A significant growth of the critical driving force is observed for varying the volume fraction of added filler particles from 0% to 12% with an increase in the fracture toughness at a given position of the cut.
- The fracture toughness of the filled rubber increases with the rise in the volume fraction of filler particles.
- On increasing the cut position, the material fracture toughness rises significantly along with the critical driving force.

The underlying theoretical framework and the findings of the present investigation may help the materialist community working in characterizing the material behavior of tires and other rubber-like materials.

References

[1] Alemán J V, Alan V Chadwick, He J,Hess M, Horie K, Richard G Jones, Kratochvíl P, Meisel I, Mita I, Moad G *et al* 2007 Definitions of terms relating to the structure and processing of sols, gels, networks, and inorganic-organic hybrid materials (iupac recommendations 2007). *Pure Appl. Chem.*, 79(10): 1801–1829

[2] Kumar D and Sarangi S 2018 Data on the viscoelastic behavior of neoprene rubber. *Data in Brief* 21: 943

[3] Kumar D, Lateefi Md M and Sarangi S 2019 A phenomenological model for the viscoelastic behaviour of natural rubber.In: *IOP Conference Series: Materials Science and Engineering*, volume 577, page 012020. IOP Publishing

[4] Ogden R W, Non-Linear Elastic Deformations. ISBN 0-486-69648-0, 1984

[5] Muhr A H 2005 Modeling the stress-strain behavior of rubber. *Rubber Chem. Technol.* 78(3): 391–425

[6] Kumar D and Sarangi S 2018 Instability analysis of an electro-magneto-elastic actuator: a continuum mechanics approach. *AIP Adv*. 8(11): 115314

[7] Lateefi Md M, Kumar D and Sarangi S 2018 Stability analysis of a hyperelastic tube under large deformation. In: *2018 International Conference on Automation and Computational Engineering (ICACE)*, pages 234–239. IEEE

[8] Kumar D and Sarangi S 2019 Electromagnetostriction under large deformation: modeling with experimental validation. *Mech. Mater.* 128: 1-10

[9] Yoda R 1998 Elastomers for biomedical applications.*J. Biomater. Sci. Polym. Ed.*, 9(6): 561–626

[10] Shanks R A *et al* 2013 General purpose elastomers: structure, chemistry, physics and performance. *Adv. Elastomers* I: 11–45

[11] Visakh P M, Thomas S, Chandra A K and Mathew A P 2013 *Advances in elastomers*. Springer

[12] Kumar D, Ghosh S, Roy S and Santapuri S 2021 Modeling and analysis of an electro-pneumatic braided muscle actuator. *J. Intell. Mater. Syst. Struct.* 32(4): 399–409

[13] Long Y and Shanks R A 1996 Pp–elastomer–filler hybrids. I. processing, microstructure, and mechanical properties. *J. Appl. Polym. Sci.* 61(11): 1877–1885

[14] Bartczak Z, Argon A S, Cohen R E and Weinberg M 1999 Toughness mechanism in semi-crystalline polymer blends: II. High-density polyethylene toughened with calcium carbonate filler particles. *Polymer* 40(9): 2347–2365

[15] Sangerano M, Pallaro E, Roppolo I and Rizza G 2009 UV-cured epoxy coating reinforced with sepiolite as inorganic filler. *J. Mater. Sci.* 44(12): 3165–3171

[16] Unal H, Mimaroglu A and Alkan M 2004 Mechanical properties and morphology of nylon-6 hybrid composites. *Polym. Int.* 53(1): 56–60

[17] Takahara A, Magome T and Kajiyama T 1994 Effect of glass fiber-matrix polymer interaction on fatigue characteristics of short glass fiber-reinforced poly (butylene terephthalate) based on dynamic viscoelastic measurement during the fatigue process. *J. Polym. Sci. Part B: Polym. Phys.* 32(5): 839–849

[18] Sau K P, Chaki T K and Khastgir D 1998 The change in conductivity of a rubber-carbon black composite subjected to different modes of pre-strain. *Compos. A Appl. Sci. Manuf.* 29(4): 363–370

[19] Joly S, Garnaud Gi, Ollitrault R, Bokobza L and Mark J E 2002 Organically modified layered silicates as reinforcing fillers for natural rubber. *Chem. Mater.* 14(10): 4202–4208

[20] Job A E, Oliveira F A, Alves N, Giacometti J A and LHC Mattoso 2003 Conductive composites of natural rubber and carbon black for pressure sensors. *Synthetic Metals* 99–100

[21] Pötschke P, Bhattacharyya A R and Janke A 2003 Morphology and electrical resistivity of melt mixed blends of polyethylene and carbon nanotube filled polycarbonate. *Polymer* 44(26): 8061–8069

[22] LeBaron P C and Pinnavaia T J 2001 Clay nanolayer reinforcement of a silicone elastomer. *Chem. Mater.* 13(10): 3760–3765

[23] Reichert W F, Göritz D and Duschl E J 1993 The double network, a model describing filled elastomers. *Polymer* 34(6): 1216–1221

[24] Farris R J 1968 The influence of vacuole formation on the response and failure of filled elastomers. *Trans. Soc. Rheol.* 12(2): 315–334

[25] Berriot J, Lequeux F, Monnerie L, Montes H, Long D and Sotta P 2002 Filler–elastomer interaction in model filled rubbers, a 1h nmr study. *J. Non-Crystalline Solids* 307: 719–724

[26] Leonard M, Wang N, Lopez-Pamies O and Nakamura T 2020 The nonlinear elastic response of filled elastomers: Experiments vs. theory for the basic case of particulate fillers of micrometer size. *J. Mech. Phys. Solids* 135: 103781

[27] Sawyers K N and Rivlin R S 1997 The trousers test for rupture. In: *Collected Papers of RS Rivlin*, pages 2643–2648. Springer

[28] Busfield J J C, Davies C K L and Thomas A G 1996 Aspects of fracture in rubber components.*Prog. Rubber Plastics Technol.* 12(3): 191–207

[29] Ahmad D, Sahu S K and Patra K 2019 Fracture toughness, hysteresis and stretchability of dielectric elastomers under equibiaxial and biaxial loading. *Polym. Testing* 79: 106038

[30] Horgan C O and Schwartz J G 2005 Constitutive modeling and the trousers test for fracture of rubber-like materials. *J. Mech. Phys. Solids* 53(3): 545–564

[31] Horgan C O and Smayda M G 2012 The trousers test for tearing of soft biomaterials. *Int. J. Solids Struct.* 49(1): 161–169

[32] Guth E 1945 Theory of filler reinforcement. *Rubber Chem. Technol.* 18(3): 596–604

[33] Waluyo S 2020 Composite dielectric elastomers modeling based on statistical mechanics. *Mech. Res. Commun.* 110: 103623

[34] Beatty M F 1987 Topics in finite elasticity: hyperelasticity of rubber, elastomers and biological tissues-with examples

[35] Rivlin R S and Saunders D W 1951 Large elastic deformations of isotropic materials vii. experiments on the deformation of rubber. *Philos. Trans. R. Soc. Lond. Series A Math. Phys. Sci.* 243(865): 251–288

[36] Bergstrom J S and Boyce M C 1999 Mechanical behavior of particle filled elastomers. *Rubber Chem. Technol.* 72(4): 633–656

[37] Chen L and Zheng Y 2012 Study on curve fitting based on least square method. *J. Wuxi Inst. Technol.* 11(5): 52–55

[38] Mahmoud W E, Al-Ghamdi A A, Al-Marzouki F and Al-Ameer S 2011 Evaluation and modeling of the mechanical behavior of carbon nanoparticle/rubber-modified polyethylene nanocomposites. *J. Appl. Polym. Sci.* 122(5): 3023–3029

[39] Zehnder A T 2013 *Griffith Theory of Fracture*, pages 1570–1573. Springer US, Boston, MA

[40] Irwin G R 1948 Fracturing of metals.*ASM, Cleveland* 147: 19–9

[41] Rivlin R S and Gr Thomas A 1953 Rupture of rubber. I. Characteristic energy for tearing. *J. Polymer Sci.* 10(3): 291–318